Do alternative inventories converge on the spatiotemporal representation of spring ammonia emissions in France?

Audrey Fortems-Cheiney[1,*], Gaëlle Dufour[1], Karine Dufossé[2,**], Florian Couvidat[3], Jean-Marc Gilliot[2], Guillaume Siour[1], Matthias Beekmann[1], Gilles Foret[1], Frederik Meleux[3], Lieven Clarisse[4], Pierre-François Coheur[4], Martin Van Damme[4], Cathy Clerbaux[4,5] and Sophie Génermont[2]

[1]Laboratoire Interuniversitaire des Systèmes Atmosphériques, UMR CNRS 7583, Université Paris Est Créteil et Université de Paris, Institut Pierre Simon Laplace, Créteil, France.

[2]Université Paris-Saclay, INRAE, AgroParisTech, UMR ECOSYS,78850 Thiverval-Grignon, France.

[3]Institut National de l'Environnement Industriel et des Risques, INERIS, 60550 Verneuil en Halatte, France.

[4]Université libre de Bruxelles, Spectroscopy, Quantum Chemistry and Atmospheric Remote Sensing (SQUARES), Brussels, Belgium.

[5]LATMOS/IPSL, Sorbonne Université, UVSQ, CNRS, Paris, France.

*now at Laboratoire des Sciences du Climat et de l'Environnement, LSCE-IPSL (CEA-CNRS-UVSQ), Université Paris-Saclay, 91191 Gif-sur-Yvette, France.

**now at UniLaSalle - Ecole des Métiers de l'Environnement, Rennes, France.

Abstract

Agriculture is the main source of ammonia (NH_3) in France, an important gaseous precursor of atmospheric particulate matter (PM). National and even more global emission inventories are known to have difficulty representing the large spatial and temporal variability inherent to atmospheric NH_3. In this study, we compare NH_3 emissions in France during the spring 2011 from one reference inventory, the TNO inventory, and two alternative inventories that account in different manners for both the spatial and temporal variabilities of the emissions: (i) the NH_3SAT satellite-derived inventory based on IASI NH_3 columns and (ii) the CADASTRE-CIT inventory that combines NH_3 emissions due to nitrogen fertilization calculated with the mechanistic model VOLT'AIR on the database of the CADASTRE_NH_3 framework and other source emissions from the CITEPA. The total spring budgets, from March to May 2011, at the national level are higher when calculated with both alternative inventories than with the reference, the difference being more marked with CADASTRE-CIT. NH_3SAT and

CADASTRE-CIT inventories both yield to large NH_3 spring emissions due to fertilization on soils with high pH in the northeastern part of France (65 ktNH_3 and 135 ktNH_3, respectively, vs 48 ktNH_3 for TNO-GEN), while soil properties are not accounted for by the TNO-GEN methodology. For the other parts of France, the differences are smaller. The timing of fertilization and associated ammonia emissions is closely related to the nitrogen requirements and hence the phenological stage of the crops, and therefore to the crop-year's specific weather conditions. Maximum emissions are observed in March for 2011 for some regions for both alternative inventories, while April is the period with maximum emissions for the reference inventory whatever the region or the year. Comparing the inventories at finer temporal resolutions, typically at daily scale, large differences are found. The convergence of alternative, independent and complementary methods on the spatiotemporal representation of the spring NH_3 emissions particularly over areas where the contribution of mineral fertilizer spreading to the spring budget is strong, encourage further developments in both prospected complementary directions, as this will help improving national NH_3 emission inventories.

1. Introduction

France is a major crop producer and a major exporter of agricultural and food products. In 2014, it produced 2%, 4%, 5%, 8%, 8% and 14% of the global production of maize, sunflower, wheat, barley, rapeseed and sugar beet, respectively [Food and Agriculture Organization of the United Nations FAO, Schauberger et al., 2018]. Through this food cultivation and also due to animal husbandry, agriculture is the main source of ammonia (NH_3) in the country. As an important gaseous precursor of particulate pollution, harmful to human life [Lelieveld et al., 2015; WHO, 2016], ammonia plays an important role in the regulation of inorganic aerosol concentrations [Erisman and Schaap, 2004, Bauer et al., 2016], and contributes to N deposition and potential exceedance of critical loads of ecosystems [Erisman et al., 2007; EEA European Environment Agency, 2014]. In order to limit air pollution, also responsible for acidification and eutrophication, the new European National Emission Ceilings Directive 2016/2284, replacing the Directive 2001/81/EC, now sets ambitious national reduction commitments for ammonia. Ammonia emissions indeed have to be reduced by 19% in 2030, compared with the 2005 levels [OJEU, 2016].

At the European scale, total NH_3 emissions are provided by the European Monitoring and Evaluation Program (EMEP) [Vestreng, 2005] or by the TNO-MACCIII [Kuenen et al., 2014] inventories that rely on national annual declarations and estimates of emission factors. Emissions are accounted for without separating fertilization and livestock. These reference inventories are widely used by the scientific community to study the impact of pollutant emissions on the chemical composition of the troposphere and on air quality. Nevertheless, uncertainties on the quantification of the NH_3 emissions are usually estimated to be between 100 and 300% of the annual budgets in the reference inventories [EMEP/EEA, 2016; Kuenen et al., 2014]. In addition, the temporal and spatial variability may not **be** well represented in the reference inventories, as the temporal profiles used do not account for meteorology, soil properties and other local conditions. Moreover, fertilizer spreading is of particular interest, as these are applied during small periods, especially during a few weeks at the end of winter and early spring. However, the exact timing of fertilizer spreading is difficult to predict, as it depends on agricultural practices and meteorological conditions, which is not taken into account in the temporal disaggregation of the reference emission inventories. Both the inaccurate temporal resolutions and the mis-representation of the spreading emissions largely explain the difficulty encountered by models to represent seasonal or daily pattern of NH_3 concentrations [Menut et al., 2012], and consequently particulate matter levels [Fortems-Cheiney et al, 2016].

To reduce these uncertainties, a better quantification of agricultural ammonia emissions and its temporal and spatial evolution is necessary. In particular, one of the challenges is to capture the right timing of fertilizer spreading at the weekly or even at the daily scale in order to reflect the effect of environmental and agronomical conditions on ammonia emissions. To this end, mechanistic models taking into account meteorological conditions, soil properties and agricultural practices, have been developed (e.g., for Denmark [Skjøth et al., 2004], for the UK [Hellsten et al., 2008], and for mineral fertilization in springtime in France [Hamaoui-Laguel et al., 2014]). Limitations for such approaches come from the fact that detailed agricultural data needed as input to such models are not available for most of the European countries. Moreover, agricultural practices of a specific country cannot be extrapolated to another country [Skjøth et al., 2011].

As an alternative to direct emission modeling, attempts have been made to constrain ammonia emissions through inverse approaches, based on ammonium wet deposition data [Paulot et al., 2014] or on satellite observed atmospheric ammonia distributions (e.g., from the Tropospheric Emission Spectrometer TES [Zhu et al., 2013; Zhang et al., 2018], from the Infrared Atmospheric Sounding Interferometer (IASI) [Fortems-Cheiney et al., 2016; Van Damme et al., 2018; Adams et al., 2019] or from the Cross-track Infrared Sounder CrIS [Adams et al., 2019; Dammers et al., 2019]). In principle, such emission estimates can be available shortly after observation. The advantage of satellite-derived estimates is also that these can be derived globally, at a high temporal scale (e.g., daily scale under clear sky). The downside of these however, is that they do not provide information on the underlying sources of the emissions (fertilizers vs husbandry), or e.g. the date of fertilization, the type of fertilizers used, the fertilization rates, etc., that could be important for the regulation of NH_3 emissions.

In this context, we compare ammonia emissions in France from inventories using the different approaches mentioned above: (i) the reference, in the sense that this is the method currently used, hereafter called TNO-GEN, is the European inventory based on the annual budgets provided by the TNO-MACCIII inventory [Kuenen et al., 2014] and on seasonal profiles from GENEMIS [Ebel et al., 1997]; (ii) a first alternative inventory, hereafter called NH_3SAT, is based on a top-down approach starting from the IASI derived NH_3 columns; (iii) the other alternative inventory, hereafter called CADASTRE-CIT, is based on a bottom-up approach quantifying NH_3 emissions due to nitrogen fertilization combining spatiotemporal data and calculations performed within the CADASTRE_NH_3 framework with the mechanistic model VOLT'AIR (Ramanantenasoa et al., [2018]; Génermont et al., [2018]) completed with livestock and other source emissions from the French Interprofessional Technical Centre for Studies on Air Pollution (CITEPA). This study aims at assessing the potential contribution of better spatial and temporal representation of fertilization-related ammonia emissions to the quality of ammonia emission inventories. The improvement is assessed in terms of total budget, spatial distribution and timing of the emissions. The study period, spring 2011 (from March, 1st to May 2011, 31st), was chosen following three criteria. Firstly, because at the time of the study, the last French agricultural data were available from AGRESTE [AGRESTE, 2014] for the agricultural year 2010-2011, allowing the application of the CADASTRE_NH_3 framework for the quantification of the spatio-temporal distribution of NH_3 emissions due to nitrogen fertilization for this crop year [Ramanantenasoa et al., 2018;Génermont et al., 2018]. Secondly, ammonia emissions are enhanced during spring in accordance with crops requirements [Skjøth et al., 2004; Ramanantenasoa et al., 2018; Génermont et al., 2018]. Finally, unlike autumn and winter months, the NH_3 spring levels are detectable with a better confidence in the IASI satellite observations [Viatte et al., 2020], allowing the extension of the preliminary work of Fortems-Cheiney et al. [2016] to deduce NH_3 emissions from the IASI satellite instrument.

The three inventories and methods to build them used for this study are presented in Section 2 and the results of the comparison are given and discussed in Section 3.

2. Inventories

The three inventories TNO-GEN, NH_3SAT and CADASTRE-CIT compared in this study are described in Table 1 and in the following sections. It is worth noting that only the CADASTRE-CIT inventory provides information on the respective contribution of fertilization and livestock emissions. The spatial and temporal resolutions of the inventories are also shown in Table 1.

Name	Spatial Resolution (latitude x longitude)	Temporal Resolution	Fertilization emissions	Livestock emissions
TNO-GEN	0.125°x0.0625°	Monthly	-	
NH_3SAT	0.5°x0.25°	Daily	-	
CADASTRE-CIT	0.015625° x0.03125°	Hourly	CADASTRE_NH_3 Ramanantenasoa et al., [2018] and Génermont et al., [2018]	
	0.007825°x0.007825°	Daily		CITEPA national emissions, temporalized according to Skøjth et al., [2011]

Table 1. *Main characteristics of the different compared inventories before their aggregation/disaggregation for the inter-comparison.*

The inter-comparison is made at the 0.5° (longitude) x 0.25° (latitude) resolution. The outputs of the TNO-GEN and the CADASTRE-CIT inventories could have consequently been aggregated or disaggregated.

2.1. TNO-GEN

In this study, the TNO-GEN combines the annual budgets provided by the TNO-MACCIII inventory and the seasonal profiles to deduce the monthly variability of NH_3 emissions. This inventory is based on official annual emission data submitted by countries to EMEP/CEIP (European Monitoring and Evaluation Programme/Centre on Emission Inventories and Projections) for air pollutants. It is the update of the TNO-MACCII inventory [Kuenen et al., 2014]. It is an inventory at 0.125°x0.0625° resolution providing annual emissions of NH_3 from the agricultural sector, without separating the contributions from fertilization and livestock. Hereafter, we use the TNO-MACIII emissions of year 2011. The seasonal profile of these emissions is prescribed according to the typical national factors provided by GENEMIS. This seasonal temporal profile used for the temporalization of emissions -the same one applied to the entire country- leads to a maximum in NH_3 emissions systematically in April over France [Ebel et al., 1997]. The emissions remain constant between days in each month and between hours in each day.

2.2. NH_3SAT

As a first alternative, a mass-balance approach, which is a common method for the quantification of short-lived species surface fluxes [Palmer et al., 2003; Jaeglé et al., 2004; Boersma et al., 2008; Lin et al., 2010] was set-up. We used it to deduce NH_3 emissions from differences between NH_3 total columns observed by the IASI instrument and simulated by the CHIMERE regional chemical transport model (CTM) using the TNO-GEN inventory as inputs data.

2.2.1 The regional CTM CHIMERE

CHIMERE simulates concentrations of gaseous and particulate chemical species [Menut et al., 2013; Mailler et al., 2017]. For this study, we used the CHIMERE version 2013a. The horizontal resolution is given as follows: 0.5° × 0.25° over 17°W/40°E–32°N/70°N, including 115 (longitude) x 153 (latitude) grid-cells. The vertical grid contains 17 layers from the surface to 200 hPa. This model is driven by the European Centre for Medium-Range Weather Forecasts global meteorological fields [Owens and Hewson, 2018]. Climatological values from the LMDz-INCA global model [Szopa et al., 2008] are used to prescribe concentrations at the lateral and top boundaries and the initial atmospheric composition in the domain. For inorganic species, aerosol thermodynamic equilibrium is achieved using the ISORROPIA model [Nenes et al., 1998].

As most of the models in the world, the parameterization of NH_3 dry deposition is unidirectional in CHIMERE. The parameterization of a bidirectional exchange with surfaces in Wichink Kruit et al. [2012] increased their yearly mean modeled LOTOS-EUROS European ammonia concentrations almost everywhere, and particularly over agricultural source areas. However, Zhu et al. [2015], with the Goddard Earth Observing System-Chemistry (GEOS-Chem) global

CTM, estimated decrease of NH_3 European concentrations in April, when the inclusion of a compensation point for vegetation is included. Further work needs to be done to better investigate the sensitivity of NH_3 concentrations to the deposition. Nevertheless, without such parameterization for bi-directional exchange, Azouz et al. [2019] assessed that regional models such as CHIMERE usually operating with large grid cell sizes simulate quite well the average NH_3 dry deposition flux over a large domain of simulation.

The evaluation of CHIMERE NH_3 and NH_4+ concentrations should be done against NH_3 (as done in Fortems-Cheiney et al., [2016]) and NH_4+ measurements. Nevertheless, to our knowledge, there is no available NH_3 measurement over France for the focused period here. There is interpretable NH_4^+ surface measurements at only one site, making the interpretation of the results difficult. NH_3 and NH_4^+ comparisons during other periods are scarce also. For instance, Tuccella et al., [2019] compared CHIMERE simulated and observed NH_4^+ at the Cabaux supersite and found average concentrations for May 2008 of 1.3 µg/m^3 for both, with a correlation coefficient of 0.52. For the Paris agglomeration between September 2009 and 2010, the modelled regional NH_4^+ burden was 1.8 µg/m^3 while the modelled one was 1.6 µg/m^3 [Petetin et al., 2016]. From June to September 2010, 83% of modelled total NH_x was gaseous, while in the model, it was only 50%, coherent with this NH_3 was underestimated especially during warmer days. Thus, it is concluded for one site and season, that particulate NH_4^+ has a low to medium impact on NH_3.

2.2.2. The IASI observations

We use data from the IASI-A instrument, flying on a low Sun-synchronous polar orbit aboard Metop satellite since October 2006, with equator crossing times of 09:30 (descending mode) and 21:30 (ascending mode) local sidereal time (LST) [Clerbaux et al., 2009, Clarisse et al., 2009]. The spatial resolution of its observations is about 12x12 km^2 at nadir. The algorithm used to retrieve NH_3 columns from the radiance spectra is described in Van Damme et al., [2017]. Several improvements have been introduced since the description of Van Damme et al., [2014] and the version v1 used in our previous study [Fortems-Cheiney et al., 2016]. In this study, we use the reanalyzed dataset ANNI-NH3-v2.2R, relying on ERA-Interim meteorological input data from the European Centre for Medium-Range Weather Forecasts (ECMWF) rather than the operationally provided Eumetsat IASI Level 2 (L2) data used for the standard near-real-time version [Van Damme et al., 2017]. We only consider land measurements from the morning overpass, as IASI is more sensitive at this time to the boundary layer, owing to more favorable thermal conditions [Clarisse et al., 2010, Van Damme et al., 2014].

The IASI total columns are averaged into "super-observations" (average of all IASI data within the 0.5°×0.25° resolution and for the given CHIMERE physical time-step of about 5/10 minutes). As suggested by Van Damme et al. [2017], we no longer use weighted averages for this purpose. We performed a sensitivity test by selecting the IASI pixels for which the retrieval error does not exceed 100%: the results about the temporal and spatial variability of the NH_3 French emissions presented in Section 3 did not significantly change, showing the robustness of the IASI NH_3 product (not shown).

The resulting monthly means of IASI NH_3 columns from March to May 2011 are shown in Figure 1 (a to c). The spatio-temporal variability -with the highest values over northeastern France in March, and over northwestern France in April- is confirmed by the IASI 10-year and by the CrIS 5-year monthly means shown in Viatte et al. [2020]. Note that the potential of IASI to provide information at high temporal resolution, up to daily scale, can be hampered by the cloud coverage as only observations with a cloud coverage lower than 10% are delivered [Van Damme et al., 2017]. To evaluate the impact of this limitation, the number of IASI super-observations used to calculate these monthly means, which represents the number of days over a month covered by IASI, is shown in Figure 1 (d to f). On average, more than half of the month is sampled by IASI during spring, except in May in the northwestern part of France. The regions showing large IASI NH_3values are consequently well sampled.

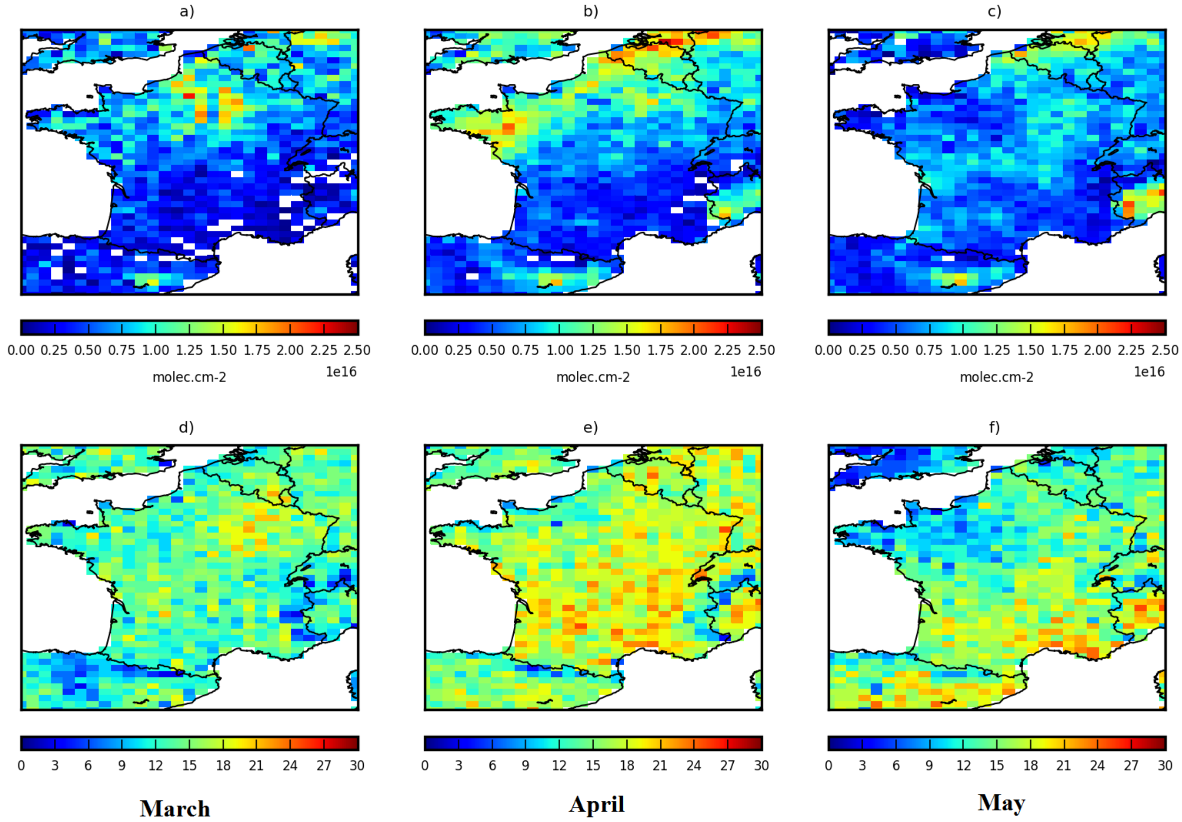

Figure 1. (*top) Monthly means of IASI "super-observations" for (a) March 2011, (b) April 2011 and (c) May 2011. Units are molec.cm*$^{-2}$. *(bottom) Total number of IASI super-observations per month in (d) March 2011, (e) April 2011 and (f) May 2011.*

2.2.3. Deducing NH_3SAT emissions

Relative differences between simulated columns by the CHIMERE regional CTM (described in Section 2.2.1, using the TNO-GEN emissions for the year 2011, described in Section 2.1) and observed IASI total columns (described in Section 2.2.2) are applied as a corrective factor to the reference emissions at daily and at grid-cell resolutions over France, from February to May 2011. As IASI "super-observations" provide one piece of information per day, the diurnal time profile of reference emissions cannot be improved: we apply the same daily correction factor to all hourly NH_3 emissions. When IASI is not available (i.e., observations with a cloud coverage higher than 10%), the correction is not applied and the emissions remain equal to the TNO-GEN ones. To compare the emissions with the CADASTRE-CIT inventory, and their respective simulations with CHIMERE, the correction is only applied over France here.

With the mass-balance approach, the transport to neighboring cells is assumed negligible following Palmer et al., [2003]. This approach has been debated by Turner et al. [2012], who found that non-local sources contribute substantially to columns of short-lived species. Li et al. [2019] evaluated the ability of both a mass-balance approach and a variational assimilation to recover known NH_3 emissions at different spatial resolutions. At a 2°x2.5° resolution, they found that both methods yielded similar values. At a 0.25°x0.3125°, the mass-balance approach led to values about 20% higher compared to the variational ones. With our 0.5°x0.25° resolution, the use of a mass-balance approach would lead to additional errors of less than about 20% for the quantification of NH_3 emissions. This uncertainty is acceptable and much lower than the uncertainty existing in the annual and national budgets provided by emission inventories [EMEP/EEA, 2016]. In this context, we choose to perform such mass-balance approach to deduce NH_3 emissions from IASI ANNI-NH_3-v2.2R super-observations. Additional uncertainty comes from the IASI observations. The IASI minimum detection limit is of about 2-3 ppbv (~4-6.10^{15}molecules.cm^{-2}) [Clarisse et al., 2010]. The signal-to-noise ratio therefore presents better performance for regions with high local concentrations (e.g., northern part of France, Figure 1) than over low local concentration areas (e.g southern parts of France, Figure 1). There is no evaluation available for the IASI ANNI-NH_3-v2.2R product used here yet.

2.3. CADASTRE-CIT

As a second alternative, a bottom-up approach was set-up based on the finest national inventories available for anthropogenic sources of ammonia. The CADASTRE_NH_3 framework provides such an inventory for organic and mineral fertilization practices. This is however not the case for the other anthropogenic sources. For livestock emissions, with the exception of the stage of effluent spreading in the field, the less detailed inventory of the French Interprofessional Technical Centre for Studies on Air Pollution CITEPA is used. To meet the objectives of better specialization and temporalization, specific procedures are applied. These inventories are completed by the TNO-GEN inventory for the emissions of the other sectors.

2.3.1. Fertilization emissions from CADASTRE_NH_3

The CADASTRE_NH_3 was implemented in order to represent in a realistic way spatio-temporal variability of French NH_3 emissions due to mineral and organic N fertilization, and is fully described in Ramanantenasoa et al. [2018] and in Génermont et al. [2018]. It has been constructed through the combined use of two types of resources: the process-based VOLT'AIR model and geo-referenced and temporally explicit databases for soil properties, meteorological conditions and N fertilization.

VOLT'AIR is a 1D process-based model predicting NH_3 emissions from N fertilizers on bare soils, from physical, chemical and biological processes [Le Cadre, 2004; Garcia et al., 2012]. It incorporates current knowledge on NH_3 volatilization after application of the main types of organic manure and mineral N fertilizers in the field. It takes into account the major factors known to influence NH_3 volatilization in the field, i.e., soil properties, weather conditions, cultural practices and properties of mineral fertilizers and organic products. It runs at an hourly time step at the field scale for a period of several weeks covering thus the entire volatilization duration of fertilization events.

Local features are attributed to each simulation units, the Small Agricultural Regions (SAR): local weather conditions (SAFRAN, Météo-France), the dominant soil type of the SAR from the European Soil Data Center (ESDC), with soil properties provided by the Harmonized World Soil Database (HWSD) of the Food and Agriculture Organization (FAO); areas cultivated in crop year 2010-2011 per crop per region derived from the European Land Parcel Identification System (LPIS, Common Agricultural Policy (CAP) regulations); Nitrogen fertilization management practices are derived from data of the national AGRESTE survey of cultural practices for arable crops and grassland (Department of Statistics and Forecasting of the French Ministry of Agriculture) [AGRESTE, 2014]. All input data required by VOLT'AIR are geographically overlaid and intersected with a Geographical Information System to generate input combinations in each SAR. Each input combination is used as the input data for a virtual 300m x 300m field for a simulation using VOLT'AIR. Exact times and dates of fertilizations are required to run VOLT'AIR, but for the sake of robustness, the statistical analysis of the survey data has been performed on the basis of two-week intervals for the date of fertilization. Fertilizations are thus randomly distributed within these two-week intervals in proportion to their respective representation following Ramanantenasoa et al. [2018]. Each simulation of NH_3 emissions is run at an hourly time step for a period of two months, starting one month before the fertilization in order to calculate soil water content at the time of application, and ending one month after fertilization, in order to cover the whole volatilization event.

About 160 000 runs with the VOLT'AIR model have been performed over the crop-year 2010-11to produce ammonia emissions per hour, per ha, per crop type, per SAR. Emissions can be aggregated at different spatial and temporal scales. At the spatial scale, they are weighted with the contribution of (i) each N fertilization management applied to each crop in each SAR and (ii) the area of the crop cultivated in the SAR. A procedure allows producing ammonia emissions at the required grid scale for the inventory comparison: it is based on cultivated areas for each crop as the key of desegregation-reagregation from the SAR to the 0.015625° x 0.03125°grid. At the temporal scale, emissions are aggregated over daily, weekly or monthly bases for the sake of comparison with TNO-GEN and NH_3SAT inventories. Volatilization taking place over several days, from few days to several weeks, one fertilization in one field contributes to ammonia emissions over several days or weeks. Weather condition effects on overall ammonia emissions is thus the result of both their effects on fertilization timing and their effects on volatilization intensity and dynamics over 30 days from fertilizer application.

As they are not available in the agricultural practice survey, N fertilizations of vegetables, fruits, and vines are not accounted for in CADASTRE_NH_3: their contribution is minor for France overall, only accounting for 5% of the total agricultural area [AGRESTE, 2010] but are important in particular regions. As the agricultural practice survey does not provide information over Corsica, this inventory is completed by the TNO-GEN inventory over this region (Figure 2).

2.3.2 Livestock emissions

As for the TNO-GEN inventory, French NH_3 emissions from livestock for the CADASTRE-CIT inventory are generated by using annual national emissions provided by CITEPA for 2011 (Figure 3a). Nevertheless, here these emissions have been spatially distributed differently than for the TNO-GEN inventory. This has been done by using the FAO Gridded Livestock of the World database with a resolution of 30 seconds of arc. The temporalization of the emissions has been performed as a function of temperature and wind speed with the parameterizations of Skøjth et al. [2011] for the different subsectors.

3. Results and discussion

First, we analyze the different contributions of livestock and of fertilization to the spring budget in the CADASTRE-CIT inventory. Then, the comparison of the two alternative inventories NH_3SAT and CADASTRE-CIT versus the reference inventory TNO-GEN, and their inter-comparison are made at different temporal and spatial resolutions. We evaluate the inventories at the national scale and at the scale of the different French administrative regions (the administrative division in France on level 2 of the unified NUTS territory classification, NUTS2, shown in Figure 2). We also analyze their spatial variability at the 0.5° (longitude) x 0.25° (latitude) resolution in order to draw a first picture of the consistency of the inventories in terms of the spring NH_3 total budget and to identify regions of interest. Finally, we focus on the temporal variability of the identified regions and discuss the agricultural practices that can influence the variability but also down to which temporal resolution the comparison of the inventories is relevant.

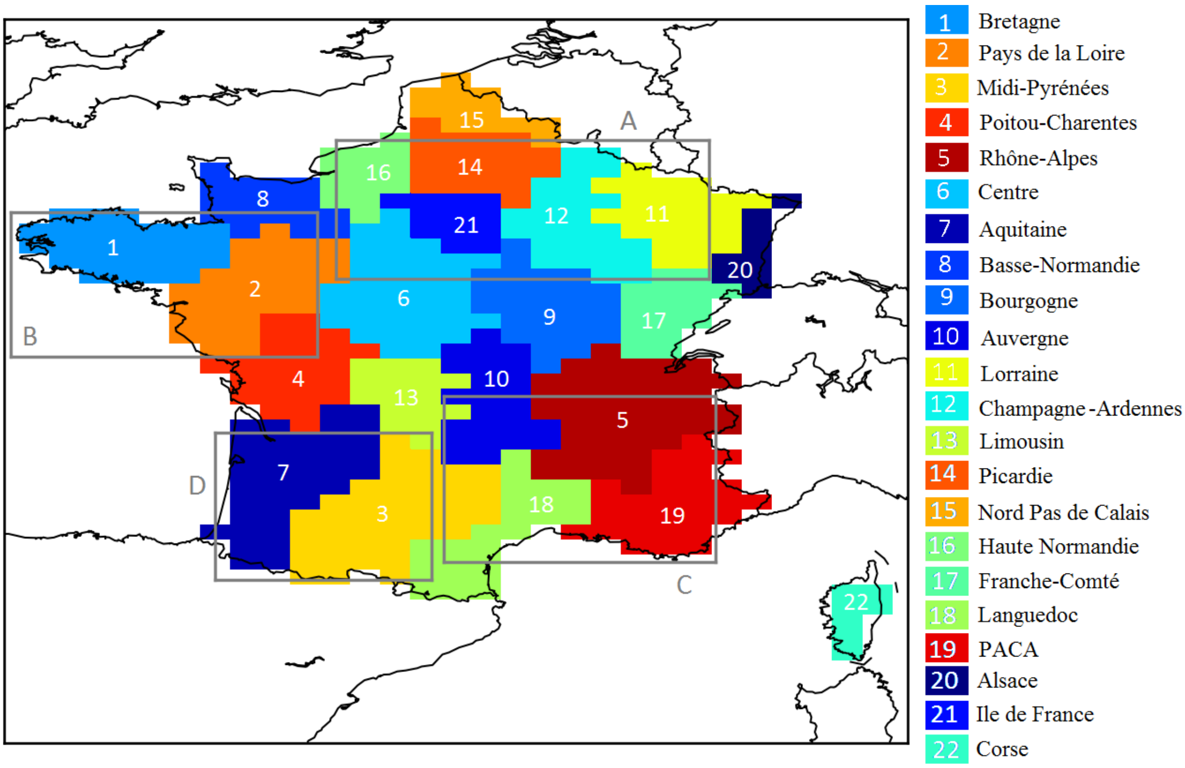

Figure 2. *Localization and names of the different French regions as taken into account in this study. The regions are listed according to the TNO-GEN annual budget, in descending order. The grey boxes A, B, C, D describe the domains we respectively call the northeastern, northwestern, southeastern and southwestern parts of France in the following.*

3.1. Respective contributions of different sources

The different contributions of livestock and of fertilization to the annual and to the spring budget in the CADASTRE-CIT inventory are shown in Figure 3. This figure shows that the contribution of fertilization to the annual French budget can be strong, with emissions occurring mainly during spring.

The different contributions of livestock and of fertilization to the spring budget in the CADASTRE-CIT inventory highlight four different domains of interest. We can see that the contribution of fertilization on the high emissions of the northeastern part of France (box A) is strong. For example, the contribution of fertilization is about 99% in the region Champagne-Ardennes, and about 85% in the region Picardie (Table 2). These emissions are mainly due to the use of mineral fertilizer over barley, sugar beet, and potato [Ramanantenasoa et al., 2018; Génermont et al., 2018]. In particular, the use of urea or nitrogen solution and the high soil pH [Hamaoui-Laguel et al., 2014; Ramanantenasoa et al., 2018; Génermont et al., 2018] - parameters not taken into account by the TNO-GEN inventory- seem to be the factors responsible for the high emissions in this domain.

The second domain of interest is the northwestern part of France (box B in Figure 3). Over this domain with high emissions, the NH_3 emissions are due in roughly equal parts to livestock (including animal housing, manure storage, and grazing) and to fertilizations, with a high use of organic manure [Ramanantenasoa et al., 2018]. Livestock farming indeed produces large amounts of livestock manure available for application on grassland and on arable crop.

The third domain of interest is the southeastern part of France (box C), showing the smallest spring NH_3 emissions. Finally, the contribution of fertilization on the emissions of the southwestern part of France (box D) is strong.

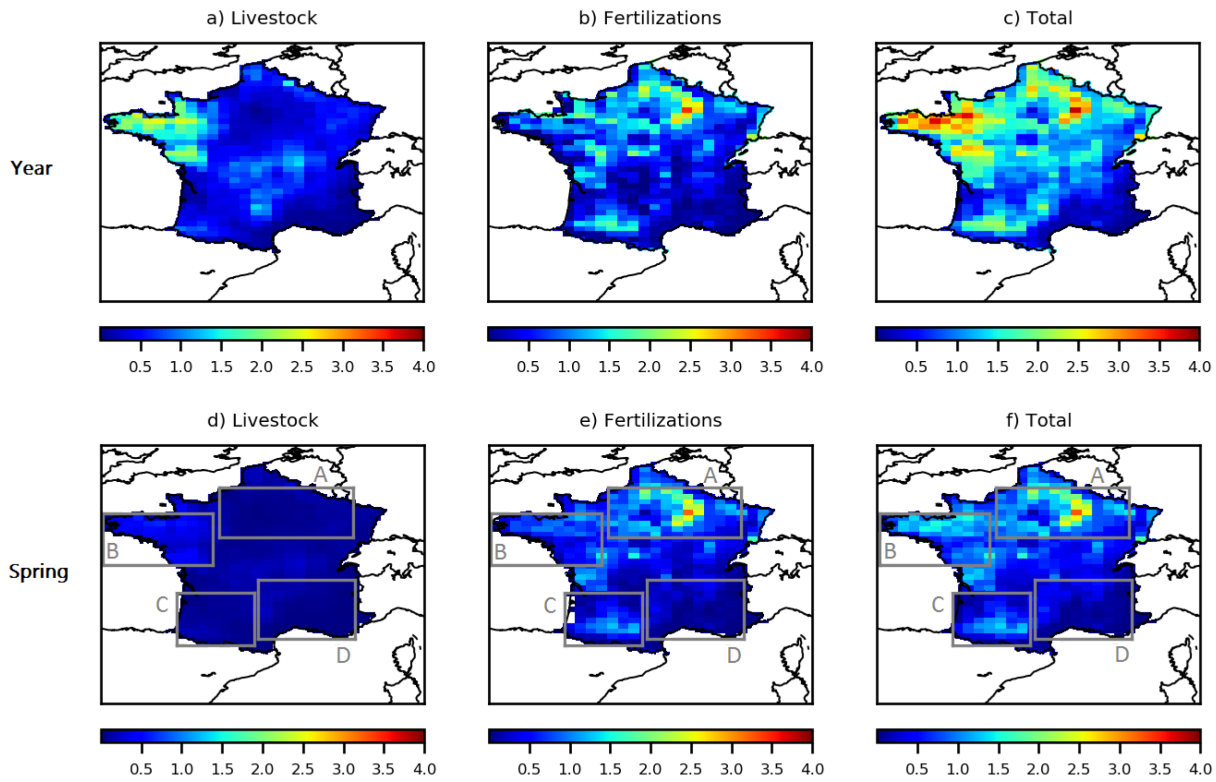

Figure 3. *top) Yearly NH_3 emissions due to a) livestock husbandry and manure storage, b) N fertilization (organic and mineral) and c) all sources in the CADASTRE-CIT inventory, in $ktNH_3$. bottom) the same for spring NH_3 emissions, from March to May 2011.*

3.2. French spring NH_3 total budget and its main spatial features

The spring NH_3 total budget is shown in Table 2 at the national scale and at the French regional scale. The French spring ammonia budgets, calculated for the period from March to May 2011, estimated by the NH_3SAT (264 ktNH_3) and the CADASTRE-CIT (354 ktNH_3) inventories are both higher than the TNO-GEN reference one (234 ktNH_3).The CADASTRE-CIT inventory estimates higher NH_3 spring emissions, by about 30%, than NH_3SAT.

The relative agreement on national budget between TNO-GEN and NH_3SAT must be nuanced as total budget values from NH_3SAT and TNO-GEN are close but large differences in the spatial distribution of the French NH_3 emissions between TNO-GEN and both NH_3SAT and CADASTRE-CIT can be observed (Figure 4).

	TNO-GEN (in ktNH_3)	**NH_3SAT (in ktNH_3)**	**CADASTRE-CIT (in ktNH_3)**	**Contribution of the fertilization to the spring budget in CADASTRE-CIT (in %)**
Regions in the northeastern part of France (box A in Figure 2)				
Champagne-Ardennes	**8**	**13 (+63%)**	**35 (+337%)**	99
Centre	**13**	**15 (+15%)**	**32 (+146%)**	81
Lorraine	**9**	**12 (+33%)**	**17 (+88%)**	80
Picardie	**8**	**12 (+50%)**	**30 (+275%)**	85
Haute-Normandie	**7**	**9 (+28%)**	**12 (+71%)**	75
Ile de France	**3**	**4 (+33%)**	**9 (+200%)**	77
Regions in the northwestern part of France (box B in Figure 2)				
Bretagne	34	34 (=)	30 (-12%)	61
Pays de la Loire	**25**	**28 (+12%)**	**29 (+16%)**	45
Regions in the southeastern part of France (box C in Figure 2)				
Rhône-Alpes	13	14 (+8%)	12 (-8%)	37
Auvergne	12	12 (=)	11 (-8%)	41
Languedoc	5	6 (+20%)	3 (-40%)	53
PACA	5	5 (=)	2 (-60%)	47
Regions in the southwestern part of France (box D in Figure 2)				
Midi-Pyrénées	18	18 (=)	26 (+44%)	60
Aquitaine	12	11 (-8%)	15 (+25%)	50
Other regions				
Alsace	**4**	**5 (+25%)**	**7 (+175%)**	87
Basse-Normandie	**11**	**15 (+36%)**	**15 (+36%)**	68

Bourgogne	**11**	**13 (+18%)**	**20 (+81%)**	55
Franche-Comté	6	6 (=)	8 (+33%)	43
Limousin	8	8 (=)	6 (-25%)	21
Nord-Pas-de-Calais	**8**	**11 (+38%)**	**10 (+25%)**	97
Poitou-Charentes	14	14 (=)	25 (+79%)	63
France				
	234	**264 (+13%)**	**354 (+51%)**	67

Table 2. *French national and regional budgets of NH_3spring emissions, from March to May 2011, in ktNH_3. The relative differences compared to the TNO-GEN are presented between brackets, in %. Regions for which the inventories NH_3SAT and CADASTRE-CIT propose the same sign of relative differences are marked in bold. The contributions of the fertilization emissions to the NH_3regional spring budget in the CADASTRE-CIT inventory are shown in %.*

Indeed, over France and for the spring budget, the spatial correlation compared to the CADASTRE-CIT inventory, which should better represent the agricultural practices and their spatial distribution, is improved when using the NH_3SAT inventory instead of using TNO-GEN (Pearson correlation coefficient r=0.78 with NH_3SAT against r=0.72 with TNO-GEN).

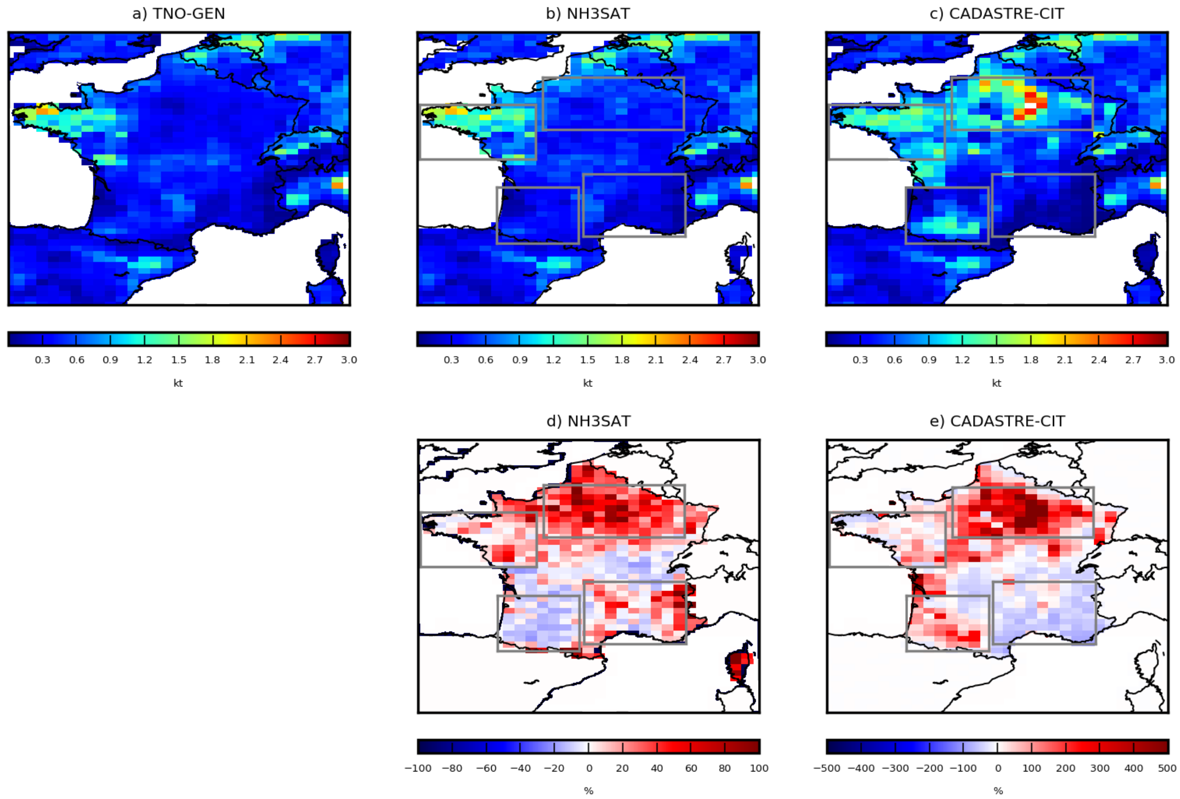

Figure 4. *French NH_3 spring emissions estimated by a) the TNO-GEN inventory, b) the NH3SAT inventory and c) the CADASTRE-CIT inventory, in ktNH_3. Relative differences of d) the NH_3SAT, and e) the CADASTRE-CIT inventories compared to the TNO-GEN inventory, in*

%, at the pixel resolution, for the period from March to May 2011. Note that the scale is different between 4b) and 4c).

The northeastern part of France presents the largest difference with the TNO-GEN inventory (48 ktNH_3) for both NH_3SAT and CADASTRE-CIT inventories (65 and 135 ktNH_3, respectively). The high emissions in the northeastern part of France are in agreement with the MASAGE_NH_3 inventory [Paulot et al., 2014], the magnitude of their annual NH_3 emissions from mineral fertilizer being calculated by combining an inventory of crop acreages, crop- and country-specific fertilizer application rates and fertilizer-, crop-, and application-specific emission factors. Emissions are higher for both NH_3SAT and CADASTRE-CIT inventories compared to TNO-GEN over the Champagne-Ardennes (+337% and +63%, respectively for CADASTRE-CIT and NH_3SAT, Table 3), Picardie (+275%, and +50%, respectively), Centre (+146% and +15%, respectively), Haute-Normandie (+71% and +28%, respectively), Lorraine (+88%, and +33%, respectively) and Ile de France regions (+200%, and +33%, respectively).

The northwestern part of France presents the largest NH_3 emissions according to the TNO-GEN inventory (Figure 4a). The TNO-GEN, NH_3SAT and CADASTRE-CIT inventories lead to similar spring budget (68, 73 and 71 ktNH_3, respectively), over this domain.

Over the southeastern part of France, CADASTRE-CIT is about 23% lower than NH_3SAT (28 and 37 ktNH_3, respectively, Table 2). One hypothesis to explain the lower NH_3 emissions in CADASTRE-CIT is that market gardening is important in this area and not taken into account in the CADASTRE-CIT inventory [Ramanantenasoa et al., 2018; Génermont et al., 2018]. Nevertheless, market gardening is not included, to our knowledge, in the TNO-GEN inventory. TNO-GEN and NH_3SAT inventories being in quite good agreement in terms of budget (35 and 37 ktNH_3, respectively, Table 2), further work is required to understand these discrepancies.

Finally, over the southwestern part of France (box D in Figure 4), IASI observations only trigger slight corrections to the TNO-GEN inventory over this area (29 and 30 ktNH_3, respectively) and CADASTRE-CIT is 36% higher than TNO-GEN and NH_3SAT (Table 2).

3.3. Temporal variability of the NH_3 emissions at the sub-seasonal scale

Monthly regional budgets have been calculated for the three inventories. Figure 5 presents the monthly variability of the NH_3 emissions from February to May 2011 for the four domains of interest presented above. February is only displayed here as a baseline to show the sharp peak of NH_3 emissions in March over some domains. The contribution of the emissions due to livestock in the CADASTRE-CIT spring budget is also given.

The TNO-GEN inventory shows rather similar NH_3 emissions from March to May for all regions, with a slight maximum in April (Figure 5a), imposed by the used GENEMIS monthly profiles for the temporalization of emissions [Ebel et al., 1997]. On the contrary, over the northeastern part of France, both NH_3SAT and CADASTRE-CIT inventories show a maximum in March, and a decrease until May by about a factor of 1.5 to 2 (Figure 5a). This maximum in March is also noticed by Tournadre et al. [2020], providing nine years of total column observations from ground-based infrared remote sensing over the Paris megacity. We calculated the monthly contribution of livestock to the NH_3 emissions based on CADASTRE-CIT, which allows one to separate this contribution from the fertilization one. As in Figure 3, Figure 5a confirms that NH_3 emissions are mainly due to fertilization in the northeastern part of France, and shows that the seasonal variation is mainly driven by this contribution. CADASTRE-CIT shows larger values than NH_3SAT which might be partly due to a possible low bias in the IASI observations [Dammers et al., 2017; Tournadre et al., 2020] combined to the fact that the TNO-GEN inventory (negatively biased compared to CADASTRE-CIT) is used as a priori for the mass balance approach with no correction applied to the a priori when IASI observations are not available.

To go further in the comparison, we analyzed the daily variability of the NH_3SAT and CADASTRE-CIT inventories -TNO-GEN representing no daily variability (Figure 6). To interpret the results, some limitations of the inventories have to be considered. For NH_3SAT, the corrections applied to the TNO-GEN emissions are only applied for clear-sky conditions when IASI observations are available. In the CADASTRE-CIT, fertilization days are randomly selected within two-week intervals of application extracted from the farm survey analysis [Ramanantenasoa et al., 2018], thus the actual day of fertilization is unknown. However, the NH_3 volatilization is continuous over several days after spreading**,** reducing the uncertainty introduced by this random selection. Moreover, the random selection is made at the field scale (see section 2.3), then spatially averaging at the CHIMERE resolution should also smoothed the random selection effect. Both effects of weather conditions on fertilization timing, on the one hand, and on volatilization intensity and dynamics at the time of application and after application, on the other hand, are realistically produced. Hence, the NH_3 volatilization is continuous over several days after spreading introducing additional smoothing.

The CADASTRE-CIT inventory presents a high day-to-day variability from March to May 2011 (Figure 6a) with several strong maxima of emissions - characteristic of emissions due to fertilizer application and a significant effect of the varying meteorological conditions. Also for NH_3SAT, day-to-day variability is large. However, NH_3SAT and CADASTRE-CIT maxima are not very well correlated. Over the first 15-days in March 2011, the high emissions occurring from the 9th to 16th in CADASTRE-CIT are not reproduced by the NH_3SAT inventory, potentially because of a lack of IASI coverage for this period (only about 40% of the domain – Figure 6a). NH_3SAT shows an emission maximum one week earlier from the 1st to 7th. This time gap in emission maxima could be explained by the random selection of fertilization days in CADASTRE-CIT. Over the last 15 days in March 2011 and over the first 15 days in April 2011, the maxima of emissions estimated by NH_3SAT and CADASTRE-CIT are more correlated, (e.g., from 7th to 11th April in CADASTRE-CIT versus from 9th to 11th in NH_3SAT). Finally, CADASTRE-CIT still shows high emissions in the last 15 days of April and in May 2011, particularly related to the use of fertilizer over corn. Despite a good coverage with IASI observations, no specific high emissions are derived from IASI for the same periods.

Over the northwestern part of France, the CADASTRE-CIT inventory is in agreement with TNO-GEN, with a slight maximum in April (Figure 5b). The NH_3SAT inventory shows a maximum in March, related to the high emissions seen during the first week of March 2011 (Figure 6b). However, the monthly differences are much smaller than for the northeastern part of France. Also for this domain, the day-to-day variabilities provided by CADASTRE-CIT and NH_3SAT are mostly uncorrelated: a strong sharp maximum of emissions during the first week of March 2011 is seen in NH_3SAT -but not reproduced in CADASTRE-CIT (Figure 6b). The highest daily emissions in CADASTRE-CIT occur during the two last weeks of April 2011 and are not reproduced by NH_3SAT.

Over the southeastern and southwestern parts of France, month-to-month variations and emission amounts are much smaller than for the two previous domains (Figures5-6c and Figures5-6d, respectively). In the southeastern part of France, NH_3SAT emissions are slightly larger than TNO-GEN and CADASTRE-CIT at the beginning of the period (February and March, Figure 5c). The fertilization contribution to CADASTRE-CIT emissions slightly decreases at the end of the period. In the southwestern part of France, NH_3SAT and TNO-GEN are very similar (Figure 5d) and CADASTRE-CIT is slightly larger at the end of spring. This increase is mainly related to fertilization emissions, the livestock contribution being stable.

Again, daily time series between both NH_3SAT and CADASTRE-CIT inventories are uncorrelated (Figures 6c, d).

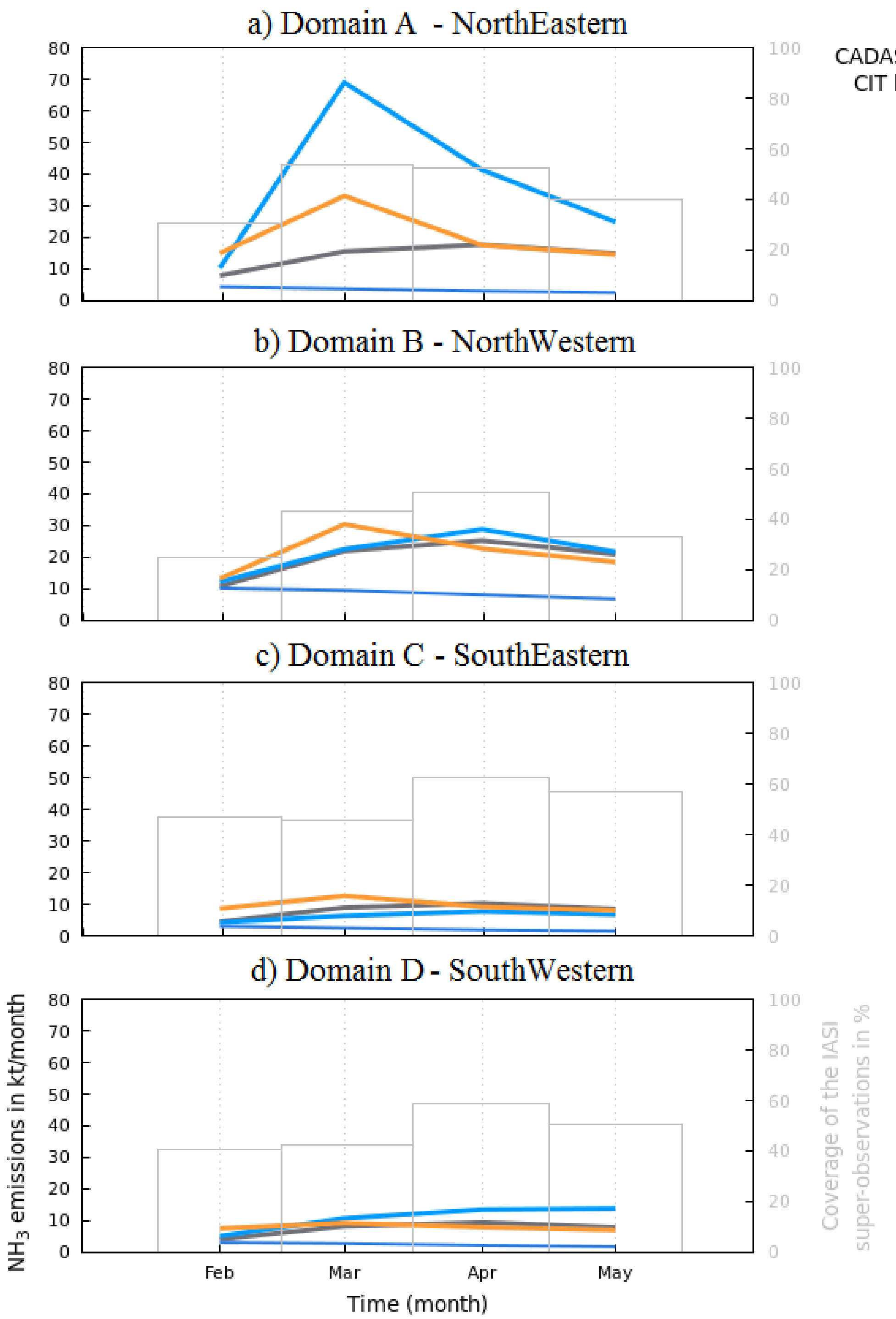

Figure 5. *Time series of monthly NH_3 emissions estimated by TNO-GEN (in black), by NH_3SAT (in orange), and by CADASTRE-CIT (in blue) inventories, from February to May 2011, for (a) domain A (northeastern), (b) domain B (northwestern), (c) domain C (southeastern), and (d)*

domain D (southwestern), as defined in Figure 2. The contribution of the emissions due to livestock in the CADASTRE-CIT monthly budgets is also given. Units are ktNH$_3$/month. The monthly regional coverage of the IASI super-observations is given in % (in grey).

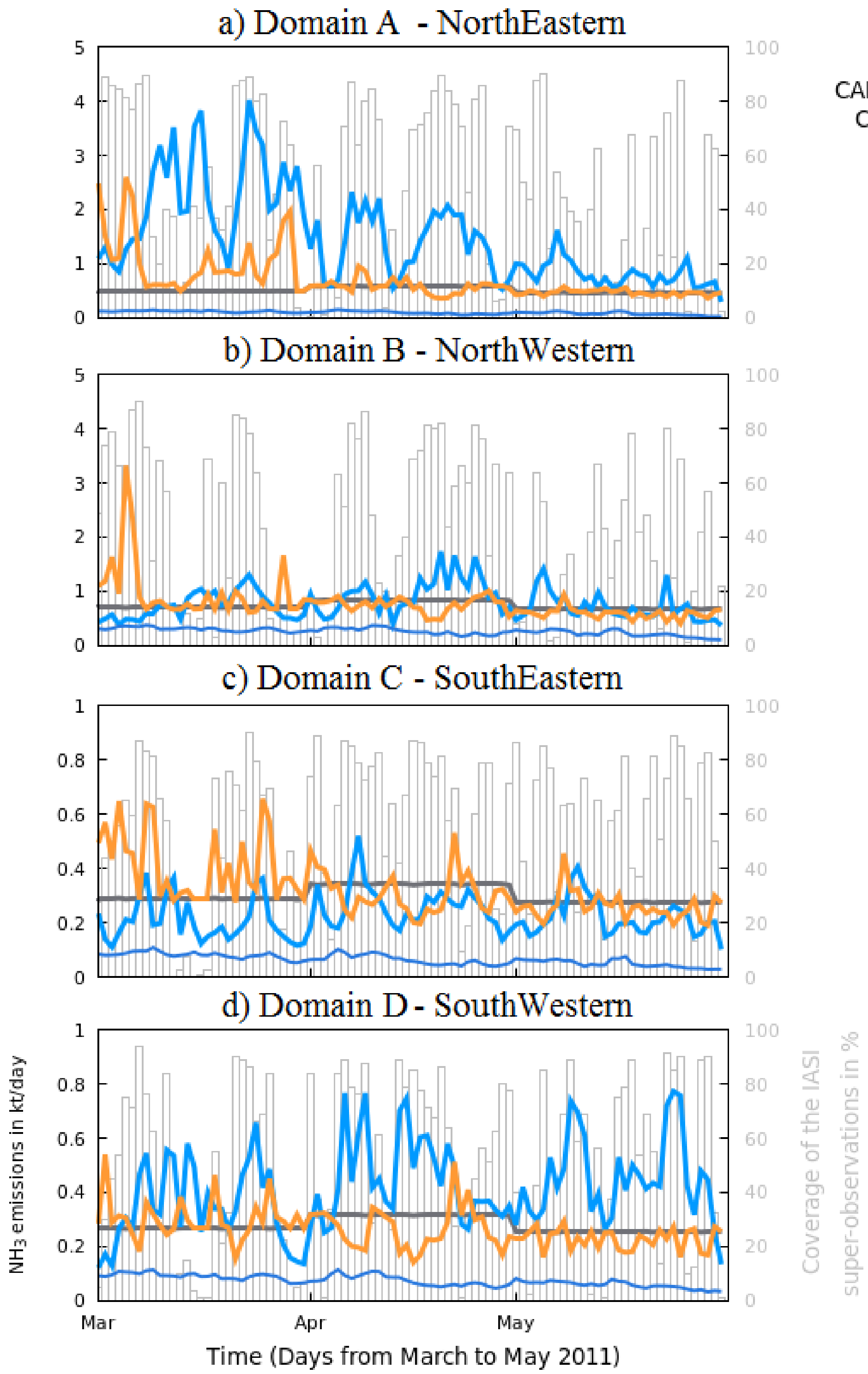

Figure 6. *Time series of daily NH$_3$ emissions estimated by TNO-GEN (in black), by NH$_3$SAT (in orange), and by CADASTRE-CIT (in blue) inventories, from March to May2011, for (a) domain A (northeastern), (b) domain B (northwestern),(c) domain C (southeastern), and (d)*

domain D (southwestern), as defined in Figure 2. Note that the scale is different between a),b) and c),d). Units are ktNH$_3$/day. The contribution of the emissions due to livestock in the CADASTRE-CIT daily variability is also given. The daily regional coverage of the IASI super-observations is given in % (in grey).

Conclusion

In this study, we performed an inter-comparison of two alternative inventories with the TNO-GEN reference inventory that quantify the French NH_3 emissions during spring 2011. One of the main conclusions of this study is that over regions with large mineral fertilizer use, like over the northeastern part of France, induced NH_3 emissions are probably considerably underestimated by the TNO-GEN reference inventory, as both the NH_3SAT (constrained by IASI observations) and CADASTRE-CIT (process level oriented), show much larger values. For instance, over northeastern France, NH_3SAT and CADASTRE-CIT show respectively a factor 1.4 and 2.8 larger spring 2011 emissions than TNO-GEN. Over the whole France, NH_3 emissions are still more than 50% larger in CADASTRE-CIT than in TNO-GEN. Average French NH_3SAT emissions are about 10% larger than TNO-GEN ones. Over the southern part of France, with a more diverse agriculture as compared to the crop intensive one in northeastern France, differences between the inventories are on the whole lower, and signs between CADASTRE-CIT / TNO-GEN and NH_3SAT / TNO-GEN corrections are often opposite for different regions.

Month-to-month variations are again much more pronounced over northeastern France and show a maximum in March for both CADASTRE-CIT and NH_3SAT. Day-to-day variations are large in CADASTRE-CIT and NH_3SAT, roughly a factor of 5 between minimal and maximal values. This shows the interest in evaluating NH_3 emissions at a daily scale because this input is required for chemistry transport modeling of particulate matter formation and thus air quality. However, time-series delivered by CADASTRE-CIT and NH_3SAT are uncorrelated for all considered regions. This result can be partly explained by the lack in IASI NH_3 column observations under partially cloudy conditions, and by the fact that available information on agricultural practices is resolved at a two weeks scale.

Yet, current results of our study have important implications for air quality modelling over Europe. The important changes in the spatial distribution of NH_3 emissions as a function of soil properties are of general concern not only for France, but for whole Europe. Soils are alkaline or neutral (pH>6) not only over North-Eastern France, but also over large parts of Italy, eastern Spain, or eastern Germany [Reuter, 2008]. Over these regions, our study suggests potentially larger NH_3 emissions than with a constant emission factor treatment, with impacts then on fine particle formation. These features should be included in “operational” emission inventories used for air quality modelling.

Thus, as a general conclusion, use of observational constrained or process-oriented emission inventories is clearly of added-value for estimating better monthly averages over French areas with intensive mineral fertilizer use, but capacity for delivering day-to-day variations is not yet proven. This warrants further studies, both refining hypotheses on days chosen by farmers for fertilizer spread out as a function of meteorological conditions, and, acquiring and using continuous surface NH_3 measurements for validating satellite or process derived NH_3 emission variability.

Competing interests

The authors declare that they have no conflict of interest.

Author Contribution

All authors have contributed to the manuscript writing (main authors A.F-C, G.D, S.G and MB). A.F-C has performed the mass-balance approach to deduce NH_3 emissions from NH_3 total columns observed by the IASI satellite instrument. K.D, J-M.G and S.G have performed the bottom-up approach providing the CADASTRE_NH_3 inventory for organic and mineral fertilization practices. F.C has compiled this CADASTRE_NH_3 inventory with livestock emissions from the CITEPA. L.C, P-F.C, M.V.D and C.C are the PIs of the IASI NH_3 product. All authors discussed the results and contributed to the final paper.

Code and Data Availability

The CHIMERE code is available here: www.lmd.polytechnique.fr/chimere/.

The IASI ANNI-NH3-v2.2R data are freely available through the AERIS database: https://iasi.aeris-data.fr/nh3/.

Acknowledgements

We acknowledge the TNO team for providing NH_3 emissions. For this study, A. Fortems-Cheiney and K. Dufossé were funded respectively by the Amp’Air and the PolQA Primequal projects, under agreement numbers ADEME 1660C0013 and 1662C0023, respectively. L.C and M.V.D are respectively research associate and postdoctoral researcher with the Belgian

F.R.S-FNRS. The authors are indebted to all those who provided input data for CADASTRE_NH_3 2010-11 crop year: the *Service de la Statistique et de la Prospective* (SSP), Department of Statistics and Forecasting of the French Ministry of Agriculture, for the French cultural practices survey, supported by a public grant overseen by the French National Research Agency (ANR) as part of the “Investissements d’avenir” program (reference: ANR-10-EQPX-17 – *Centre d’Accès Sécurisé aux Données* – CASD); Météo-France for the data on weather conditions; the *Agence de Service et de Paiement* (ASP) and the *Observatoire du Développement Rural* (ODR) service unit for data on Land Parcel Identification System (LPIS) for France. The authors are also grateful to M.M.J. Ramanantenasoa for her technical assistance, funded by the Cadastre_NH_3 project under agreement number ADEME 1081C0031. IASI is a joint mission of EUMETSAT and the Centre National d’Etudes Spatiales (CNES, France). The authors acknowledge the AERIS data infrastructure for providing access to the IASI data in this study. This research has been supported by the Belgian State Federal Office for Scientific, Technical and Cultural Affairs (Prodex arrangement IASI.FLOW). This work was granted access to the HPC resources of TGCC under the allocation A0050107232 made by GENCI.

References

Adams, C., McLinden, C. A., Shephard, M. W., Dickson, N., Dammers, E., Chen, J., Makar, P., Cady-Pereira, K. E., Tam, N., Kharol, S. K., Lamsal, L. N., and Krotkov, N. A.: Satellite-derived emissions of carbon monoxide, ammonia, and nitrogen dioxide from the 2016 Horse River wildfire in the Fort McMurray area, Atmos. Chem. Phys., 19, 2577–2599, https://doi.org/10.5194/acp-19-2577-2019, 2019.

AGRESTE Pratiques culturales 2006. In “Agreste Les Dossiers”, n°8- July 2010, pp.86, 2010.

AGRESTE Enquête Pratiques culturales 2011. In “Agreste Les Dossiers”, n°21- July 2014, pp.70, 2014.

Azouz, N. et al: Comparison of spatial patterns of ammonia concentration and dry deposition flux between a regional Eulerian chemistry-transport model and a local Gaussian plume model, Air Quality, Atmosphere & Health (2019) 12:719–729 https://doi.org/10.1007/s11869-019-00691-y, 2019.

Bauer, S. E., Tsigaridis, K., and Miller, R.: Significant atmosphericaerosol pollution caused by world food cultivation, Geophys.Res. Lett., 43, 5394–5400, 2016.

Boersma K. F., Jacob D. J., Bucsela E. J., Perring A. E., Dirksen R., van der A R. J., Yantosca R. M., Park R. J., Wenig M. O., & Bertram T. H.:Validation of OMI tropospheric NO_2 observations during INTEX-B and application to constrain NO_x emissions over the eastern United States and Mexico. Atmospheric Environment, 42(19), 4480–4497. 10.1016/j.atmosenv.2008.02.004, 2008.

CITEPA, Centre Interprofessionnel Techniqued'Etudes de la Pollution Atmosphérique, Format SECTEN, https://www.citepa.org/fr/air-et-climat/polluants/aep-item/ammoniac, last access September 2019.

Clarisse, L., Clerbaux, C., Dentener, F., Hurtmans,D., and Coheur, P.: Global ammonia distribution derived from infrared satellite observations, Nat. Geosci., 2, 479–483, 2009.

Clarisse, L., Shephard, M., Dentener, F., Hurtmans, D., Cady-Pereira, K., Karagulian, F., Van Damme, M., Clerbaux, C., and Coheur, P.-F.: Satellite monitoring of ammonia: A case study of the San Joaquin Valley, J. Geophys.Res., 115, D13302, https://doi.org/10.1029/2009JD013291, 2010.

Clerbaux, C., Boynard, A., Clarisse, L., George, M., Hadji-Lazaro, J., Herbin, H., Hurtmans, D., Pommier, M., Razavi, A., Turquety, S., Wespes, C., and Coheur, P.-F.: Monitoring of atmospheric composition using the thermal infrared IASI/MetOp sounder, Atmos. Chem. Phys., 9, 6041–6054, doi:10.5194/acp-9-6041-2009, 2009.

Dammers, E., Shephard, M. W., Palm, M., Cady-Pereira, K., Capps, S., Lutsch, E., Strong, K., Hannigan, J. W., Ortega, I., Toon, G. C., Stremme, W., Grutter, M., Jones, N., Smale, D., Siemons, J., Hrpcek, K., Tremblay, D., Schaap, M., Notholt, J., and Erisman, J. W.: Validation of the CrIS fast physical NH_3 retrieval with ground-based FTIR, Atmos. Meas. Tech., 10, 2645–2667, https://doi.org/10.5194/amt-10-2645-2017, 2017.

Dammers, E., McLinden, C. A., Griffin, D., Shephard, M. W., Van Der Graaf, S., Lutsch, E., Schaap, M., Gainairu-Matz, Y., Fioletov, V., Van Damme, M., Whitburn, S., Clarisse, L., Cady-Pereira, K., Clerbaux, C., Coheur, P. F., and Erisman, J. W.: NH_3emissions from large point sources derived from CrIS and IASI satellite observations, Atmos. Chem. Phys., 19, 12261–12293, https://doi.org/10.5194/acp-19-12261-2019, 2019.

Ebel, A., Friedrich, R., and Rodhe, H.: Tropospheric Modelling and Emission Estimation. Transport and Chemical Transformation of Pollutants in the Troposphere, chap. GENEMIS: Assessment, Improvement, and Temporal and Spatial Disaggregation of European Emission Data, Springer, Berlin, Germany, 1997.

EEA European Environment Agency: Effects of air pollution on European ecosystems - Past and future exposure of European freshwater and terrestrial habitats to acidifying and eutrophying air pollutants, https://www.eea.europa.eu/publications/effects-of-air-pollution-on, Technical Report, 2014.

EMEP European Monitoring and Evaluation Program/EEA European Environment Agency, 2016, Air pollutant emission inventory guidebook Uncertainties, 2016.

Erisman, J.W. and Schaap, M.: The need for ammonia abatement with respect to secondary PM reductions in Europe, Environ. Pollut., 129,159–163, https://doi.org/10.1016/j.envpol.2003.08.042, 2004.

Erisman, J.W., Bleeker, A., Galloway, J., and Sutton, M.S.: Reduced nitrogen in ecology and the environment, Environ. Pollut., 150, 1, 140-149, https://doi.org/10.1016/j.envpol.2007.06.033,2007.

Fortems-Cheiney A.,Dufour, G., Hamaoui-Laguel, L., Foret, G., Siour, G., Van Damme, M., Meleux, F., Coheur, P.-F., Clerbaux, C., Clarisse, L., Wallash, M. and Beekmann, M.: Unaccounted variability in NH_3 agricultural sources detected by IASI contributing to European spring haze episode, Geophysical Research Letters, 43, 10, 5475–5482, https://doi.org/10.1002/2016GL069361, 2016.

Garcia, L., Génermont, S., Bedos, C., Simon, N. N., Garnier, P., Loubet, B., and Cellier, P.: Accounting for Surface Cattle Slurry in Ammonia Volatilization Models: The Case of Volt'Air. Soil Science Society of America Journal, 76, 2184. DOI:10.2136/sssaj2012.0067, 2012.

Génermont, S., Ramanantenasoa, M.M.J., Dufossé, K., Maury, O., Mignolet, C., Gilliot, J.-M. : Data on spatio-temporal representation of mineral N fertilization and manure N application as well as ammonia volatilization in French regions for the crop year 2005/06, Data in Brief 21:1119-1124. https://doi.org/10.1016/j.dib.2018.09.119, 2018.

Hamaoui-Laguel, L., Meleux , F., Beekmann, M., Bessagnet, B., Genermont, S., Cellier, P., Letinois, L.: Improving ammonia emissions in air quality modelling for France. Atmospheric Environment, 92, 584–595, doi: 10.1016/j.atmosenv.2012.08.002, 2014.

Hellsten, S., U. Dragosits, C.J. Place, M. Vieno, J. Dore, T.H. Misselbrook, Y.S. Tang, M.A. Sutton: Modelling the spatial distribution of ammonia emissions in the UK, Environmental Pollution (Barking, Essex: 1987), 154 (2008), pp. 370–379, 2008.

Jaeglé, L., R. V. Martin, K. Chance, L. Steinberger, T. P. Kurosu, D. J. Jacob, A. I. Modi, V. Yoboué, L. Sigha-Nkamdjou, and C. Galy-Lacaux, Satellite mapping of rain-induced nitric oxide emissions from soils, J. Geophys. Res., 109, D21310, doi:10.1029/2004JD004787, 2004.

Kuenen, J. J. P., Visschedijk, A. J. H., Jozwicka, M., and Denier van der Gon, H. A. C.: TNO-GEN-MACC_II emission inventory; a multi-year (2003–2009) consistent high-resolution European emission inventory for air quality modelling, Atmos. Chem. Phys., 14, 10963-10976, https://doi.org/10.5194/acp-14-10963-2014, 2014.

Le Cadre, E. : "Modélisation de la volatilisation d'ammoniac en interaction avec les processus chimiques et biologiques du sol: le modèle Volt'Air." Doctoral thesis, ABIES ; UMR INRA INAPG Environnement et Grandes Cultures de Grignon. pp. 315., 2004. http://infodoc.agroparistech.fr/index.php?lvl=notice_display&id=48284

Lelieveld, J., Evans, J.S., Fnais, M., Giannadaki, D. and Pozzer, A.: The contribution of outdoor air pollution sources to premature mortality on a global scale, Nature, 367-371, doi:10.1038/nature15371, 2015.

Li et al: Assesing the iterative finite difference mass balance and 4D-Var methods to derive ammonia emissions over North America using synthetic observations, J. Geoph. Res.,https://doi.org/10.1029/2018JD030183, 2019.

Lin, J. T., M. B. McElroy, and K. F. Boersma: Constraint of anthropogenic NOx emissions in China from different sectors: A new methodology using multiple satellite retrievals, Atmos. Chem. Phys., 10, 63–78, doi:10.5194/acp-10-63-2010, 2010.

Mailler, S., Menut, L., Khvorostyanov, D., Valari, M., Couvidat, F., Siour, G., Turquety, S., Briant, R., Tuccella, P., Bessagnet, B., Colette, A., Létinois, L., Markakis, K., and Meleux, F.: CHIMERE-2017: from urban to hemispheric chemistry-transport modeling, Geosci. Model Dev., 10, 2397–2423, https://doi.org/10.5194/gmd-10-2397-2017, 2017.

Menut, L., Goussebaile, A., Bessagnet B., Kyvorostiyanov, D., and Ung, A.: Impact of realistic hourly emissions profiles on air pollutants concentrations modelled with CHIMERE, Atmospheric Environment, 49, 233-244, 2012.

Menut, L., Bessagnet, B., Khvorostyanov, D., Beekmann, M., Blond, N., Colette, A., Coll, I., Curci, G., Foret, G., Hodzic, A., Mailler, S., Meleux, F., Monge, J.-L., Pison, I., Siour, G., Turquety, S., Valari, M., Vautard, R., and Vivanco, M. G.: CHIMERE 2013: a model for regional atmospheric composition modelling, Geosci. Model Dev., 6, 981-1028, doi:10.5194/gmd-6-981-2013, 2013.

Nenes, A., Pandis, S.N., and Pilinis, C.: Continued development and testing of a new thermodynamic aerosol module for urban and regional air quality models, Atmospheric Environment, 33, 1553–1560, 1999.

OJEU, Official Journal of the European, Union Directive (EU) 2016/2284 of the European Parliament and of the Council of 14 December 2016 on the reduction of national emissions of certain atmospheric pollutants, amending Directive 2003/35/EC and repealing Directive 2001/81/EC, 344, 17.12.2016, p. 1–31, http://data.europa.eu/eli/dir/2016/2284/oj, 2016.

Owens, R. G. and Hewson, T.: ECMWF Forecast User Guide,https://doi.org/10.21957/m1cs7h, 2018.

Paulot, F., D. J. Jacob, R. W. Pinder, J. O. Bash, K. Travis, and D. K. Henze: Ammonia emissions in the United States, European Union, and China derived by high-resolution inversion of ammonium wet deposition data: Interpretation with a new agricultural emissions inventory (MASAGE_NH3), J. Geophys. Res. Atmos., 119, 4343–4364, doi:10.1002/2013JD021130, 2014.

Palmer, P.I., Jacob, D.J., Fiore, A.M., Martin, R.V., Chance, K., and Kurosu, T.P.: Mapping isoprene emissions over North America using formaldehyde column observations from space, J. Geophys. Res., 108, D6, doi:10,1029/2002JD002153, 2003.

Petetin, H., Sciare, J., Bressi, M., Gros, V., Rosso, A., Sanchez, O., Sarda-Estève, R., Petit, J.-E., and Beekmann, M.: Assessing the ammonium nitrate formation regime in the Paris megacity and its representation in the CHIMERE model, Atmos. Chem. Phys., 16, 10419–10440, https://doi.org/10.5194/acp-16-10419-2016, 2016.

Ramanantenasoa M.M.J., Gilliot J.-M., Mignolet C., Bedos C., Mathias E., Eglin T., Makowski D., Génermont S. : A new framework to estimate spatio-temporal ammonia emissions due to nitrogen fertilization in France. Science of the Total Environment, 645:205-219. https://doi.org/10.1016/j.scitotenv.2018.06.202, 2018.

Reuter, H.I., Lado, L.R., Hengl, T. and Montanarella, L.: Continental-scale digital soil mapping using European soil profile data: soil pH, Hamburger Beiträge zur Physischen Geographie und Landschaftsökologie – 92 Heft 19/2008, pp. 91-102, 2008.

Schauberger, B et al: Yield trends, variability and stagnation analysis of major crops in France over more than a century, Nature, doi:10.1038/s41598-018-35351-1, 2018.

Skjøth, C. A., Geels, C., Berge, H., Gyldenkærne, S., Fagerli, H., Ellermann, T., Frohn, L. M., Christensen, J., Hansen, K. M., Hansen, K., and Hertel, O.: Spatial and temporal variations in ammonia emissions – a freely accessible model code for Europe, Atmos. Chem. Phys., 11, 5221-5236, doi:10.5194/acp-11-5221-2011, 2011.

Szopa, S., Foret, G., Menut, L., and Cozic, A.: Impact of large scale circulation on European summer surface ozone: consequences for modeling, Atmospheric Environment, 43, 1189–1195,doi:10.1016/j.atmosenv.2008.10.039, 2008.

Tournadre, B., Chelin, P., Ray, M., Cuesta, J., Kutzner, R. D., Landsheere, X., Fortems-Cheiney, A., Flaud, J.-M., Hase, F., Blumenstock, T., Orphal, J., Viatte, C., and Camy-Peyret, C.: Atmospheric ammonia (NH_3) over the Paris megacity: 9 years of total column observations from ground-based infrared remote sensing, Atmos. Meas. Tech., 13, 3923–3937, https://doi.org/10.5194/amt-13-3923-2020, 2020.

Tuccella, P.; Menut, L.; Briant, R.; Deroubaix, A.; Khvorostyanov, D.; Mailler, S.; Siour, G.; Turquety, S. Implementation of Aerosol-Cloud Interaction within WRF-CHIMERE Online Coupled Model: Evaluation and Investigation of the Indirect Radiative Effect from Anthropogenic Emission Reduction on the Benelux Union. *Atmosphere* 2019, *10*, 20, 2019.

Turner, A.J., Henze, D.F., Martin, R.V.andHakami, A.: The spatial extent of source influences on modeled columns concentrations of short-lived species, Geophysical Research Letters, 39, L12806, doi:10.1029/2012GL051832, 2012.

Van Damme, M., Clarisse, L., Heald, C. L., Hurtmans, D., Ngadi, Y., Clerbaux, C., Dolman, A. J., Erisman, J. W., and Coheur, P. F.: Global distributions, time series and error characterization of atmospheric ammonia (NH3) from IASI satellite observations, Atmos. Chem. Phys., 14, 2905–2922, doi:10.5194/acp-14-2905-2014, 2014.

Van Damme, M., Whitburn, S., Clarisse, L., Clerbaux, C., Hurtmans, D., and Coheur, P.-F.: Version 2 of the IASI NH3 neural network retrieval algorithm: near-real-time and reanalysed datasets, Atmos. Meas. Tech., 10, 4905-4914, https://doi.org/10.5194/amt-10-4905-2017, 2017.

Van Damme, M., Clarisse, L., Whitburn, S., Hadji-Lazaro, J., Hurtmans, D., Clerbaux, C., and Coheur, P.-F.: Industrial and agricultural ammonia point sources exposed, Nature, Volume 564, 99-103, 2018.

Vestreng, V., Breivik, K., Adams, M., Wagner, A., Goodwin, J., Rozovskaya, O., and Oacyna, J. . Inventory Review 2005 - Emission Data reported to CLRTAP and under the NEC Directive - Initial review for HMs and POPs .EMEP Status report, Norwegian Meteorological Institute, Oslo, 2005.

Viatte, C., Wang, T., Van Damme, M., Dammers, E., Meleux, F., Clarisse, L., Shephard, M. W., Whitburn, S., Coheur, P. F., Cady-Pereira, K. E., and Clerbaux, C.: Atmospheric ammonia variability and link with particulate matter formation: a case study over the Paris area, Atmos. Chem. Phys., 20, 577–596, https://doi.org/10.5194/acp-20-577-2020, 2020.

Wichink Kruit, R. J., M. Schaap, F. J. Sauter, M. C. van Zanten, and W. A. J. van Pul: Modeling the distribution of ammonia across Europe including bi-directional surface-atmosphere exchange, Biogeosciences, 9, 5261–5277, doi:10.5194/bg-9-5261-2012, 2012.

Zhang, L., Chen, Y., Zhao, Y., Henze, D. K., Zhu, L., Song, Y., Paulot, F., Liu, X., Pan, Y., Lin, Y., and Huang, B.: Agricultural ammonia emissions in China: reconciling bottom-up and top-down estimates, Atmos. Chem. Phys., 18, 339–355, https://doi.org/10.5194/acp-18-339-2018, 2018.

Zhu, L., Henze, D.K., Cady-Pereire, K.E, Shepard, M.W., Luo, M., Pinder, R.W., Bash, J.O. and Jeong, G.-R.: Constraining U.S. ammonia emissions using TES remote sensing observations and the GEOS-Chem adjoint model, J. Geophys. Res, 118, 1-14, doi:10.1002/jgrd.50166, 2013.

Zhu, L., D. Henze, J. Bash, G.-R. Jeong, K. Cady-Pereira, M. Shephard, M. Luo, F. Paulot, and S. Capps: Global evaluation of ammonia bidirectional exchange and livestock diurnal variation schemes, Atmos. Chem. Phys., 15, 12,823–12,843, doi:10.5194/acp-15-12823-2015, 2015.